Title

Osteoprotegerin reduces osteoclast resorption activity without affecting osteogenesis on nanoparticulate mineralized collagen scaffolds

Journal

Science Advances, 5(6)

ISSN

2375-2548

Authors

Ren, Xiaoyan
Zhou, Qi
Foulad, David
et al.

Publication Date

2019-06-07

DOI

10.1126/sciadv.aaw4991

Peer reviewed

CELL BIOLOGY

Osteoprotegerin reduces osteoclast resorption activity without affecting osteogenesis on nanoparticulate mineralized collagen scaffolds

Xiaoyan Ren[1,2,3], Qi Zhou[1,2,3], David Foulad[1,2,3], Aleczandria S. Tiffany[4], Marley J. Dewey[5], David Bischoff[2], Timothy A. Miller[1,2], Russell R. Reid[6], Tong-Chuan He[7], Dean T. Yamaguchi[2], Brendan A. C. Harley[4,8], Justine C. Lee[1,2,3]*

The instructive capabilities of extracellular matrix–inspired materials for osteoprogenitor differentiation have sparked interest in understanding modulation of other cell types within the bone regenerative microenvironment. We previously demonstrated that nanoparticulate mineralized collagen glycosaminoglycan (MC-GAG) scaffolds efficiently induced osteoprogenitor differentiation and bone healing. In this work, we combined adenovirus-mediated delivery of osteoprotegerin (AdOPG), an endogenous anti-osteoclastogenic decoy receptor, in primary human mesenchymal stem cells (hMSCs) with MC-GAG to understand the role of osteoclast inactivation in augmentation of bone regeneration. Simultaneous differentiation of osteoprogenitors on MC-GAG and osteoclast progenitors resulted in bidirectional positive regulation. AdOPG expression did not affect osteogenic differentiation alone. In the presence of both cell types, AdOPG-transduced hMSCs on MC-GAG diminished osteoclast-mediated resorption in direct contact; however, osteoclast-mediated augmentation of osteogenic differentiation was unaffected. Thus, the combination of OPG with MC-GAG may represent a method for uncoupling osteogenic and osteoclastogenic differentiation to augment bone regeneration.

INTRODUCTION

Materials inspired by bone-specific extracellular matrix (ECM) components have generated great enthusiasm in regenerative technologies because of their abilities to instruct osteoprogenitor differentiation. In addition, recent attention to the effects on osteoclast activation has suggested the potential for modulation of resorption within the host microenvironment via alterations of the receptor activator of nuclear factor κB (RANK), RANK ligand (RANKL), and osteoprotegerin (OPG) axis (*1*).

The RANK/RANKL/OPG axis serves an important role in osteoclast regulation and bone homeostasis (*1*, *2*). The activation of RANK, a tumor necrosis factor superfamily receptor originally identified in T lymphocytes and osteoblasts, via its cognate ligand RANKL is required for osteoclast differentiation and activation (*3*, *4*). Murine genetic models have shown that both RANK and RANKL deficiencies resulted in osteopetrosis because of a complete absence of osteoclasts (*5*, *6*). In the craniofacial skeleton, RNA interference using small interfering RNAs (siRNAs) specific for RANK has been shown to fuse patent cranial sutures in ex vivo cultures (*2*). OPG, the soluble decoy receptor for RANKL, is the major endogenous negative regulator of the pathway. In contrast to the RANK- and RANKL-deficient mice, OPG knockouts exhibit profound osteoporosis (*6*, *7*). Because of the direct relationship between the RANK/RANKL/OPG axis and osteoclast activation, targeted therapies against the axis are under investigation for fracture healing and other conditions requiring a net osteogenic state (*8*). Similar to other immune cells such as lymphocytes, in vivo activation of osteoclasts proceeds with two signals. While the RANK/RANKL/OPG axis is undeniably the major signal, co-stimulation via receptors such as osteoclast-associated receptor (OSCAR) contributes to homeostasis and may be deranged in pathologic circumstances (*9*, *10*).

The importance of osteoclast homeostasis in normal bone physiology suggests that bone regeneration is likely to be affected by the regulatory mechanisms of osteoclast activity. Components of ECM-based materials have been reported to both affect osteogenic differentiation and negatively or positively regulate osteoclastogenesis (*11*). As the most abundant protein within bone ECM, most ECM-inspired materials for bone regeneration are based on collagen I (*11*). However, the ligands for OSCAR, a costimulatory molecule for osteoclast maturation, are collagens I, II, and III (*9*). Thus, collagen-based materials intrinsically provide costimulation for osteoclast activation, potentially lowering the threshold for resorption. Collagen-based osteoclast costimulation is likely able to be offset with the negative osteoclast regulatory effects of certain glycosaminoglycan (GAG) species, as well as the inorganic components of bone ECM. Salbach-Hirsch and colleagues (*12*) extensively evaluated sulfated GAG (sGAG) coatings and found an increased osteogenic differentiation of primary murine mesenchymal stem cells and simultaneously diminished osteoclast activity, in part through sequestration of OPG. The mechanism for which GAGs or sGAGs influence osteoclastogenesis remains to be elucidated, although their work suggested that sulfation status may differentially affect osteoclast activity. Inorganic ions, specifically calcium and phosphate, have been the most extensively described ECM components that contribute to osteoclast action. High levels of extracellular calcium ions, such as during bone remodeling, negatively regulate podosomal

[1]Division of Plastic and Reconstructive Surgery, UCLA David Geffen School of Medicine, Los Angeles, CA 90095, USA. [2]Research Service, Greater Los Angeles VA Healthcare System, Los Angeles, CA 90073, USA. [3]UCLA Molecular Biology Institute, Los Angeles, CA 90095, USA. [4]Department of Chemical and Biomolecular Engineering, University of Illinois at Urbana-Champaign, Urbana, IL 61801, USA. [5]Department of Materials Science and Engineering, Institute for Genomic Biology, University of Illinois at Urbana-Champaign, Urbana, IL 61801, USA. [6]Section of Plastic and Reconstructive Surgery, University of Chicago, Chicago, IL 60637, USA. [7]Department of Orthopaedic Surgery, University of Chicago, Chicago, IL 60637, USA. [8]Carl R. Woese Institute for Genomic Biology, University of Illinois at Urbana-Champaign, Urbana, IL 61801, USA.
*Corresponding author. Email: justine@ucla.edu

assembly and resorption via entry through the L-type voltage–gated calcium channels (*13*). Similarly, high levels of extracellular inorganic phosphate inhibit RANKL-induced osteoclast activity in a manner dependent on the sodium phosphate cotransporter (*14*). Recently, the signaling mechanisms induced by inorganic ions in the context of materials have been characterized in greater detail, and further modulation may be of great utility in regenerative technologies (*15*, *16*). Using a combination biphasic silicified and calcified collagen material, Jiao *et al.* (*17*) demonstrated the up-regulation of OPG gene expression during osteogenic differentiation that was not present to the same degree in monophasic silicified collagen scaffolds or calcified collagen scaffolds. Signaling pathways responsible for osteogenesis and osteoclast inhibition of the biphasic silicified and calcified collagen material were regulated by different intracellular mediators.

Our group previously demonstrated that a nanoparticulate mineralized collagen glycosaminoglycan (MC-GAG) scaffold induced efficient mineralization of bone marrow–derived primary human mesenchymal stem cells (hMSCs) and primary rabbit bone marrow stromal cells via autogenous activation of the bone morphogenetic protein receptor (BMPR) signaling pathway through phosphorylation of small mothers against decapentaplegic-1/5 (p-Smad1/5) (*18*–*22*). Furthermore, we demonstrated that MC-GAG scaffold induced in vivo rabbit calvarial regeneration without the addition of exogenous growth factors or progenitor cells (*21*). We recently reported that MC-GAG scaffold demonstrated both direct and indirect inhibitory effects on osteoclast viability, proliferation, and activation (*23*). In comparison to its nonmineralized collagen glycosaminoglycan (Col-GAG) scaffold counterpart, MC-GAG scaffolds directly reduced viability and proliferation of primary osteoclast precursors. MC-GAG scaffolds also induced hMSCs to express higher levels of OPG during osteogenic differentiation via intracellular signaling pathways distinct from those governing osteogenic differentiation. Combining these findings suggests two concepts: (i) ECM-based materials for skeletal regeneration must account for both osteogenesis and osteoclastogenesis and (ii) differences in regulatory mechanisms evoked by nonmineralized versus mineralized collagen scaffolds may provide a route to disconnect physiologic osteoblast and osteoclast coupling. In this work, we evaluate the addition of an adenovirus-mediated OPG (AdOPG) expression in primary hMSCs with MC-GAG scaffolds to promote osteogenesis and augment osteoclast inhibition.

RESULTS

AdOPG transduction of primary hMSCs differentiated on Col-GAG and MC-GAG does not affect cell viability or proliferation

Recently, we reported that MC-GAG induces hMSCs to up-regulate OPG at higher levels than Col-GAG, suggesting a potential role for MC-GAG in simultaneously regulating the host resorptive capacity in the local microenvironment during bone regeneration. However, the amount of OPG protein expressed by hMSCs differentiated on MC-GAG was only significantly higher within the first 10 days of differentiation. Thus, we hypothesized that a prolongation of OPG expression may augment the antiresorptive capabilities of MC-GAG.

In an effort to augment anti-osteoclastogenic activities induced by MC-GAG, primary bone marrow–derived hMSCs ($CD105^+CD166^+CD29^+CD44^+CD14^-CD34^-CD45^-$) were transduced with AdOPG. Control and AdOPG-transduced hMSCs were cultured in osteogenic differentiation medium for 7 and 14 days and evaluated for infection efficiency, OPG expression, and effects on cell viability and proliferation (Fig. 1). Using the coexpressed red fluorescent protein (RFP) as an indicator, AdOPG transduction resulted in a 35% infection efficiency based on cell counting with a maximum amount of protein expression on Western blot analysis at a multiplicity of infection (MOI) of 200 (Fig. 1B).

Before evaluating long-term scaffold mineralization, the viability and proliferation of hMSCs were confirmed by measuring the mitochondrial dehydrogenase activity using the WST-1 (water-soluble tetrazolium salt 1) colorimetric assay. hMSC viability and proliferation were not found to be significantly different in control versus AdOPG-infected cells in two-dimensional (2D) cultures after 3 weeks of transduction (Fig. 1C). To confirm that cells were viable in long-term 3D cultures, we seeded control and AdOPG on Col-GAG and MC-GAG and differentiated them for 8 weeks in osteogenic differentiation medium (Fig. 1D). Again, hMSC cell viability and proliferation were found to be equivalent between control and AdOPG hMSCs on Col-GAG or MC-GAG with no statistically significant differences between the materials.

AdOPG transduction changes RANKL/OPG homeostasis in primary hMSCs differentiated on Col-GAG and MC-GAG

Because of the known importance of the OPG to RANKL-relative protein ratios in influencing bone homeostasis, we next evaluated the relative expression of OPG to RANKL in control and AdOPG-infected cells. Control and AdOPG-infected cells were induced to undergo osteogenic differentiation on Col-GAG and MC-GAG for 14 days, and quantitative real-time reverse transcription polymerase chain reaction (qRT-PCR) was performed to assess OPG and RANKL gene expression (Fig. 2, A and B). No statistically significant differences were found in OPG or RANKL gene expression between control cells on either material. In the presence of AdOPG, OPG gene expression increased more than 30-fold in cells cultured on either scaffold, while no differences in RANKL expression was noted.

Protein expression was next evaluated using both Western blot and enzyme-linked immunosorbent assay (ELISA) of OPG and RANKL expression over 56 days (Fig. 2, C to F). On Western blot analysis, we detected two dominant isoforms of RANKL including a band at 35 kDa, as well as a higher–molecular weight band near 45 kDa, which may reflect expression of different splice variants, similar to reports by several other investigators (*24*, *25*). Densitometry was used to quantify the relative expression of OPG and RANKL, and the RANKL/OPG protein expression ratio over 56 days was evaluated (Fig. 2E). As Western blots were performed on the total protein of the scaffolds, the RANKL/OPG ratio derived represented the total cellular and scaffold-bound protein. A statistically significant difference was found in the RANKL/OPG protein expression ratios between the groups [$F(3,24) = 19.35$, $P < 0.001$]. In both Col-GAG and MC-GAG, AdOPG expression lowered the RANKL/OPG protein expression ratio as expected ($P < 0.001$). In control hMSCs, Col-GAG displayed a higher RANKL/OPG ratio compared to MC-GAG ($P < 0.001$).

In addition to scaffold-bound protein, we evaluated RANKL and OPG in culture supernatants using ELISAs to calculate the secreted RANKL/OPG ratio (Fig. 2F). Similar to total protein RANKL/OPG ratios, a statistically significant difference was found [$F(3,20) = 60.56$, $P < 0.001$]. Unlike the total protein of the scaffolds, the secreted RANKL/OPG ratio was higher in MC-GAG compared to Col-GAG

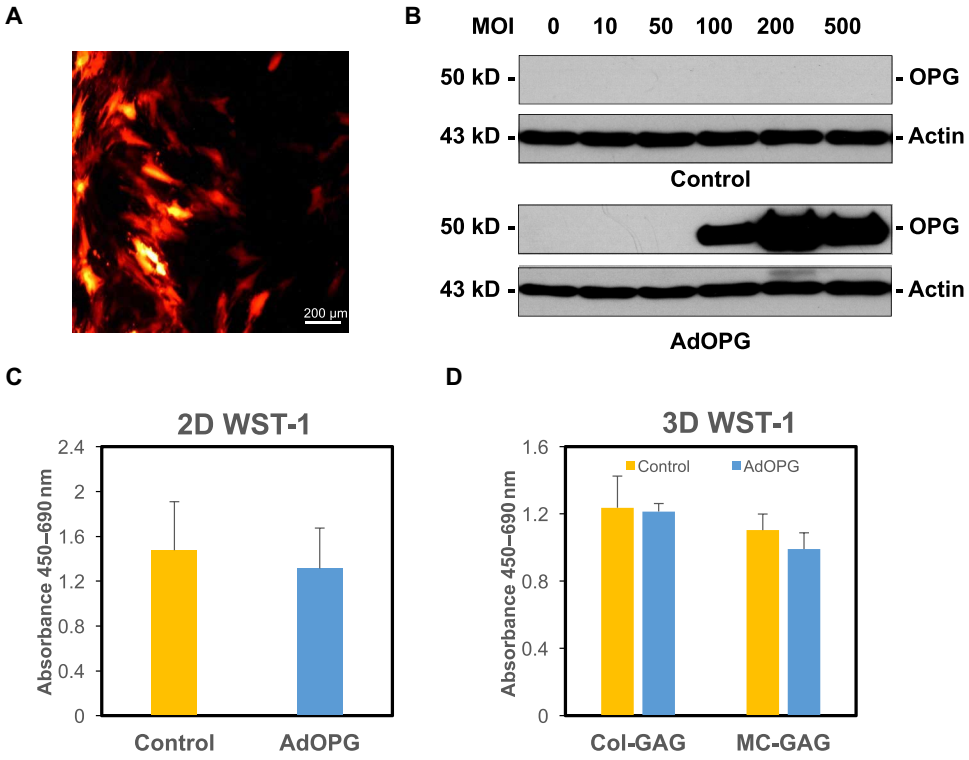

Fig. 1. AdOPG transduction of primary hMSCs differentiated on Col-GAG and MC-GAG does not affect cell viability or proliferation. (**A**) Photomicrograph of AdOPG-transduced primary hMSCs in 2D cultures after 7 days. (**B**) Western blot of primary hMSCs transduced with control or AdOPG viruses for 7 days on 2D cultures at varying MOI. (**C** and **D**) WST-1 proliferation and viability assays of primary hMSCs transduced with control of AdOPG viruses at (**C**) 3 weeks in 2D cultures and (**D**) 8 weeks on Col-GAG or MC-GAG. Mean values are shown in bars, with error bars representing SD.

($P < 0.001$) in control cells. Expression of AdOPG diminished the RANKL/OPG ratio compared to control cells on MC-GAG ($P < 0.001$), whereas less of an effect was observed for Col-GAG. Together, AdOPG significantly reduces the RANKL/OPG ratio at both the levels of gene and protein expression. For the alterations in RANK/OPG protein ratios, the difference is primarily manifested in cellular or scaffold-bound protein rather than secreted protein.

AdOPG does not affect hMSC mineralization on Col-GAG or MC-GAG

Two reports have suggested that OPG may have capabilities to induce osteogenic differentiation and mineralization in osteoprogenitor cells separate from its effects on osteoclasts and osteoclast precursors (*26*, *27*). To evaluate whether AdOPG directly affects mineralization in our system, we evaluated control and AdOPG-infected hMSCs undergoing osteogenic differentiation on Col-GAG and MC-GAG for expression of osteogenic markers, activation of osteogenic signaling pathways, and matrix mineralization (Fig. 3). At 14 days of culture, no significant differences in runt-related transcription factor 2 (RUNX2) or osteopontin (OPN) gene expression were found between control and AdOPG cells on Col-GAG or MC-GAG (Fig. 3, A and B).

We previously showed that both Col-GAG and MC-GAG depended on the activation of the BMPR signaling pathway via p-Smad1/5 for osteogenic differentiation and matrix mineralization (*22*). Thus, to evaluate the contribution of AdOPG to the activation of intracellular signaling pathways that contribute to mineralization on Col-GAG and MC-GAG, we performed the Western blots analyses of control and AdOPG-infected hMSCs undergoing osteogenic differentiation on Col-GAG or MC-GAG on total protein lysates over 8 weeks (Fig. 3, C and D). No significant differences in p-Smad1/5 activation were detected in the absence or presence of AdOPG. MC-GAG, as we previously demonstrated, induced substantially more p-Smad1/5 compared to Col-GAG.

We also quantified matrix mineralization using microcomputed tomography (μCT) analysis (Fig. 3, E and F). Again, no significant differences between control and AdOPG hMSCs were detected on either Col-GAG or MC-GAG. Similar to our previous reports, MC-GAG demonstrated more mineralization than Col-GAG with or without AdOPG.

Indirect osteoclast cocultures augment mineralization in hMSCs undergoing mineralization on MC-GAG in the absence or presence of AdOPG

To understand the effects of MC-GAG on human osteoclasts (hOCs), we used two coculture techniques: indirect and direct. Indirect cocultures were performed to isolate the effects of hOCs on hMSCs and vice versa without the confounding effects of scaffold resorption from direct contact and to understand the paracrine effects between the two cell types (Fig. 4A). Direct cocultures were devised for the purposes of understanding the net effects of the system with cells and materials in direct contact with each other. For indirect cocultures, Col-GAG or MC-GAG scaffolds were cultured in an 8-μm Transwell insert with and without hMSCs seeded on the materials (upper chamber). In the lower chamber, human primary pre-osteoclasts were seeded on a calcium phosphate–coated plate

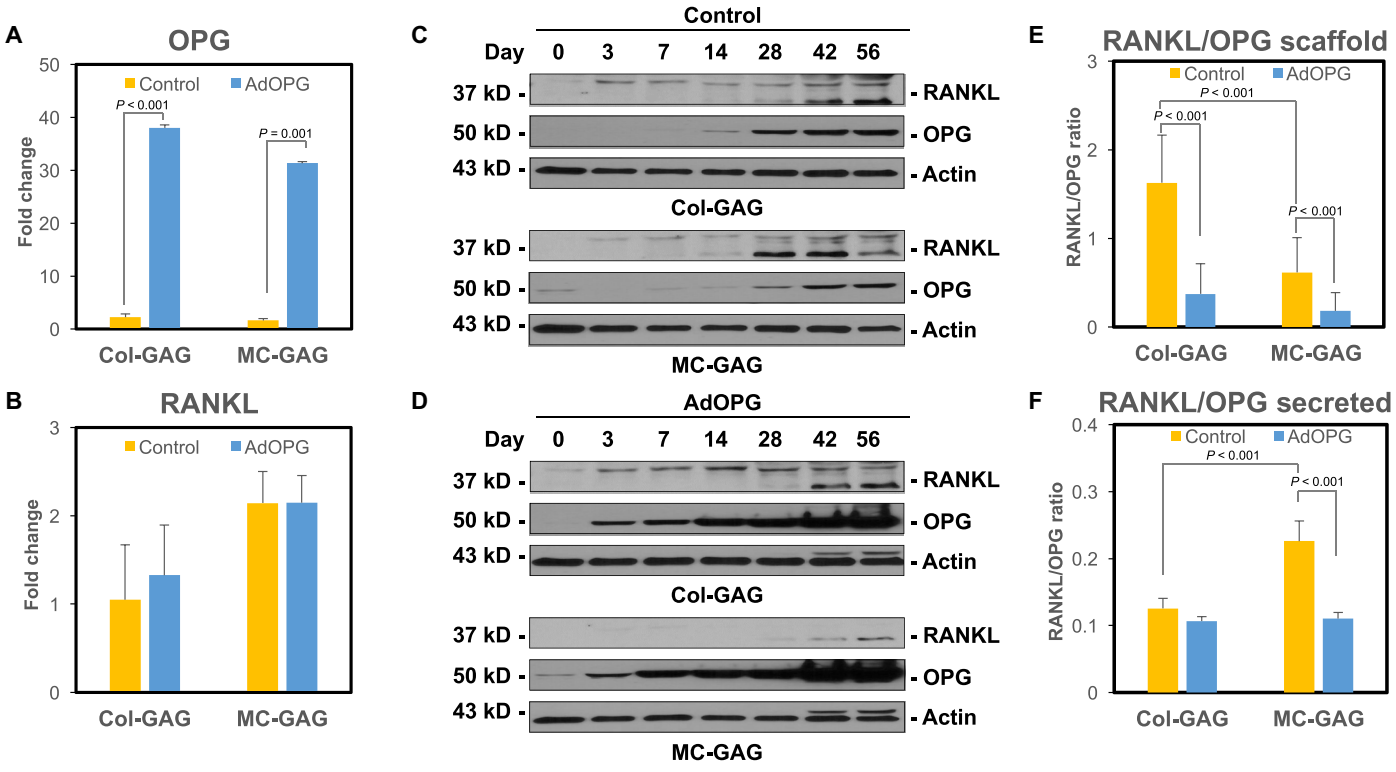

Fig. 2. AdOPG transduction changes RANKL/OPG homeostasis in primary hMSCs differentiated on Col-GAG and MC-GAG. qRT-PCR of control or AdOPG-transduced primary hMSCs cultured on Col-GAG or MC-GAG materials for 14 days in osteogenic differentiation medium for (**A**) OPG and (**B**) RANKL ($n = 3$). Western blot of (**C**) control or (**D**) AdOPG-transduced primary hMSCs cultured on Col-GAG or MC-GAG materials for 56 days in osteogenic differentiation medium for RANKL, OPG, and β-actin. Average RANKL/OPG protein expression ratio based on (**E**) densitometric analysis of RANKL and OPG Western blot bands or (**F**) ELISA of culture supernatants over 8 weeks. Mean values are shown in bars, with error bars representing SD. Significant post hoc comparisons following analysis of variance (ANOVA) indicated with *P* values.

where resorptive activity may be evaluated. Cocultures were concurrently differentiated with medium supplemented with RANKL, macrophage colony-stimulating factor (M-CSF), β-glycerophosphate, ascorbic acid, and dexamethasone.

In the indirect coculture system, the effects on hMSCs were first evaluated. After 21 days of culture, we subjected the Transwell inserts (upper chambers) to WST-1 assay (Fig. 4B). Statistically significant differences in viability and proliferation were found between hMSCs of the different groups [$F(7,18) = 81.36$, $P < 0.001$]. Empty Col-GAG or MC-GAG scaffolds without hMSCs cocultured with osteoclasts displayed no evidence of cell viability or proliferation as expected ($P < 0.001$ compared to any other conditions). No differences were found between hMSCs cultured without osteoclasts (hMSC only) or control hMSCs cocultured with osteoclasts (control hMSC/OC) on either material. With AdOPG, hMSCs cultured on MC-GAG demonstrated a decrease in viability and proliferation compared to Col-GAG in a statistically significant fashion ($P = 0.03$).

To determine the amount of soluble OPG in the coculture system, we performed ELISAs over the entirety of the coculture period and compared them to an osteoclast-only negative control (Fig. 4C). Differences between the cultures were found to be statistically significant [$F(4,15) = 552.37$, $P < 0.001$]. Osteoclasts did not display any significant amount of OPG secretion as expected. In control cells, hMSCs on MC-GAG produced significantly more endogenous OPG compared to Col-GAG at day 7 ($P < 0.001$) and day 10 ($P = 0.02$). Multiple comparisons of any control time point versus any AdOPG-infected time point for either material displayed significantly higher amounts of OPG in AdOPG-infected cells ($P < 0.001$ for all conditions).

We evaluated mineralization after 3 weeks of coculture using μCT scanning (Fig. 4, D and E). Overall, differences in mineralization were found to be present [$F(7,26) = 26.48$, $P < 0.001$]. An increase in osteogenic differentiation occurred in control hMSC cocultures with differentiating hOCs (control hMSC/OC) compared to hMSC single cultures (hMSC only) on MC-GAG materials ($P < 0.001$). Although a mild increase in mineralization was evident qualitatively and quantitatively on Col-GAG in cocultures versus single cultures, this difference did not reach statistical significance. In MC-GAG, the increase in mineralization for cocultures with AdOPG compared to hMSC-only single cultures remained significant ($P = 0.02$). In combination, indirect cocultures of differentiating hMSCs with hOCs resulted in positive regulation of osteogenic differentiation manifested by mineralization, particularly on MC-GAG. This increase in mineralization is largely unaffected by AdOPG transduction.

Indirect cocultures with AdOPG-transduced hMSCs on MC-GAG diminish hOC resorptive activity

In the same indirect cocultures, we also evaluated the effects on osteoclasts (Fig. 4, F and G). Following removal of the Transwell inserts, the lower chamber consisting of hOCs was subjected to WST-1 assay and found to have statistically significant differences on analysis of variance (ANOVA) [$F(6,21) = 9.23$, $P < 0.001$]. An increase in

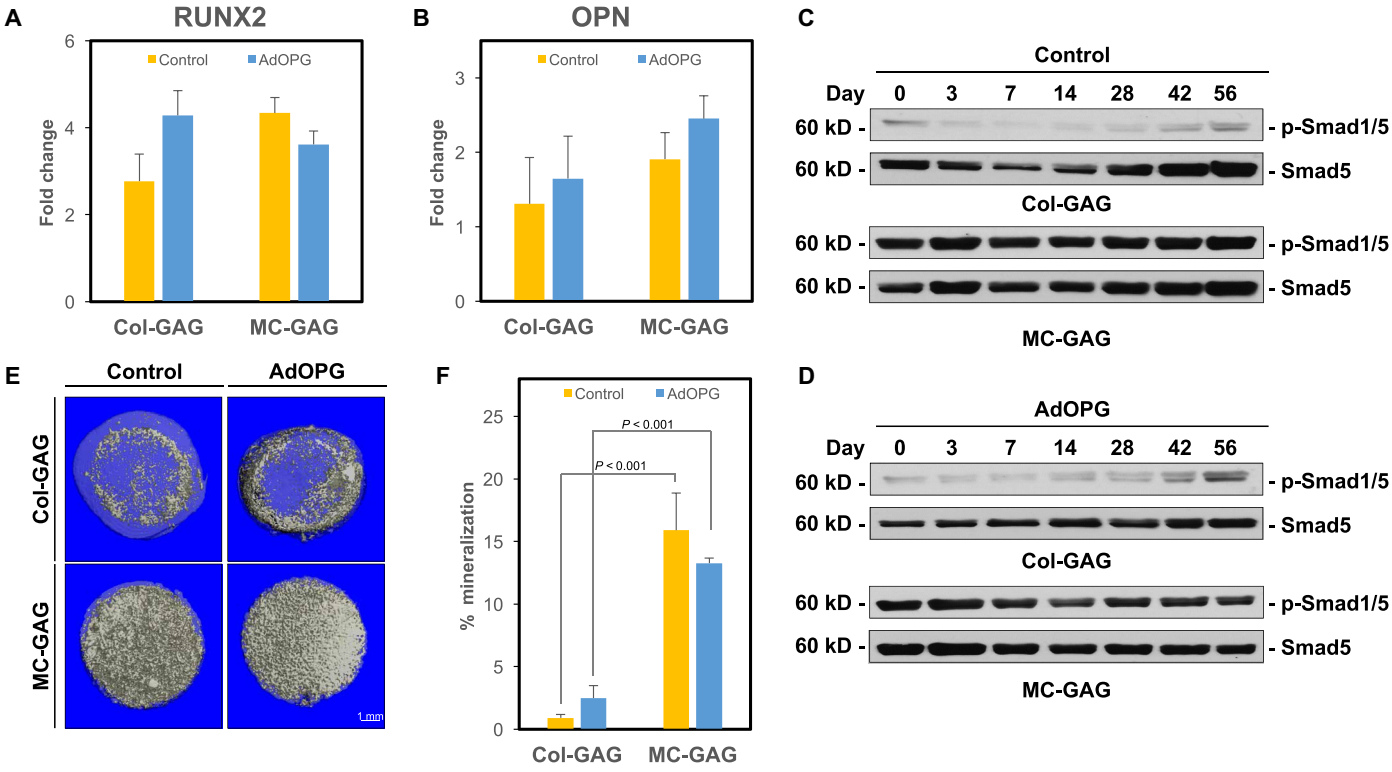

Fig. 3. AdOPG does not affect hMSC mineralization on Col-GAG or MC-GAG. qRT-PCR of control or AdOPG-transduced primary hMSCs cultured on Col-GAG or MC-GAG materials for 14 days in osteogenic differentiation medium for (**A**) RUNX2 and (**B**) OPN ($n = 3$). Western blot of (**C**) control or (**D**) AdOPG-transduced primary hMSCs cultured on Col-GAG or MC-GAG materials for 56 days in osteogenic differentiation medium for Smad5 and p-Smad1/5. (**E**) Representative μCT images and (**F**) quantitative analysis of control or AdOPG-transduced primary hMSCs cultured on Col-GAG or MC-GAG for 8 weeks ($n = 3$). Bars represent means, and error bars represent SD. Significant post hoc comparisons following ANOVA indicated with *P* values.

viability and proliferation or hOCs occurred in cocultures with control hMSCs on Col-GAG or MC-GAG ($P = 0.02$ and $P < 0.001$, respectively). AdOPG-transduced hMSCs diminished viability and proliferation of hOCs compared to control hMSCs on MC-GAG ($P = 0.03$). Minimal differences in hOC viability were detected on Col-GAG with hMSCs transduced with AdOPG.

Resorptive activity of the hOCs was also characterized and found to have significant differences via ANOVA [$F(6,17) = 15.34$, $P < 0.001$; Fig. 4G]. hOC-mediated resorption significantly increased in cocultures of hMSCs on Col-GAG ($P = 0.001$) or MC-GAG ($P = 0.002$) compared to hOC single cultures. In AdOPG-transduced hMSCs, hOC-mediated resorption diminished on both materials compared to control hMSCs; however, only the decrease in MC-GAG reached statistical significance ($P < 0.001$). In combination, these data suggest that differentiating hMSCs increase the viability, proliferation, and resorptive capabilities of hOCs on either nonmineralized or mineralized Col-GAG materials. While cocultures with AdOPG-transduced hMSCs mildly reduced hOC viability, proliferation, and resorption on Col-GAG, MC-GAG demonstrated a significantly greater effect.

Direct contact of AdOPG-transduced hMSCs on Col-GAG and MC-GAG with osteoclasts diminishes the proliferation and resorption activity of osteoclasts

Next, the effects on osteoclasts were evaluated in a direct coculture system. hOCs were first plated on a calcium phosphate–coated plate. Two hours after seeding, hMSCs seeded on Col-GAG or MC-GAG were transferred to each well in direct contact with hOCs. Cocultures were simultaneously differentiated with medium supplemented with RANKL, M-CSF, β-glycerophosphate, ascorbic acid, and dexamethasone. After 14 days of culture, we removed the respective scaffolds and subjected the osteoclasts to WST-1 assay (Fig. 5A). Statistically significant differences between the cultures were noted [$F(6,14) = 22.48$, $P < 0.001$]. In the presence of empty Col-GAG, the viability and proliferation were not significantly different from osteoclasts differentiated alone (OC only). As we previously reported, empty MC-GAG materials did reduce osteoclast viability and proliferation (*23*). Between control versus AdOPG-transduced hMSCs on either material, both viability and proliferation were diminished in the presence of AdOPG.

We assessed osteoclast differentiation and activity using tartrate-resistant acid phosphatase (TRAP) staining and resorption pit assays, respectively (Fig. 5, B and C). Under all conditions, with the exception of the negative control, TRAP activity was detected, indicating that osteoclasts were present. Osteoclast activity, detected by resorption pits of the inorganic crystalline calcium phosphate coating of the plate, demonstrated significant differences between the groups. In the presence of empty Col-GAG, a mild decrease in resorption was elicited, which was rescued with the addition of control hMSCs. In MC-GAG, a significant decrease in resorptive abilities was seen, which was also improved with the addition of control hMSCs. In both cases, osteoclast resorption was completely inhibited when transduced with AdOPG.

Quantification of the total resorption pit areas demonstrated significant differences in resorption activity between the conditions

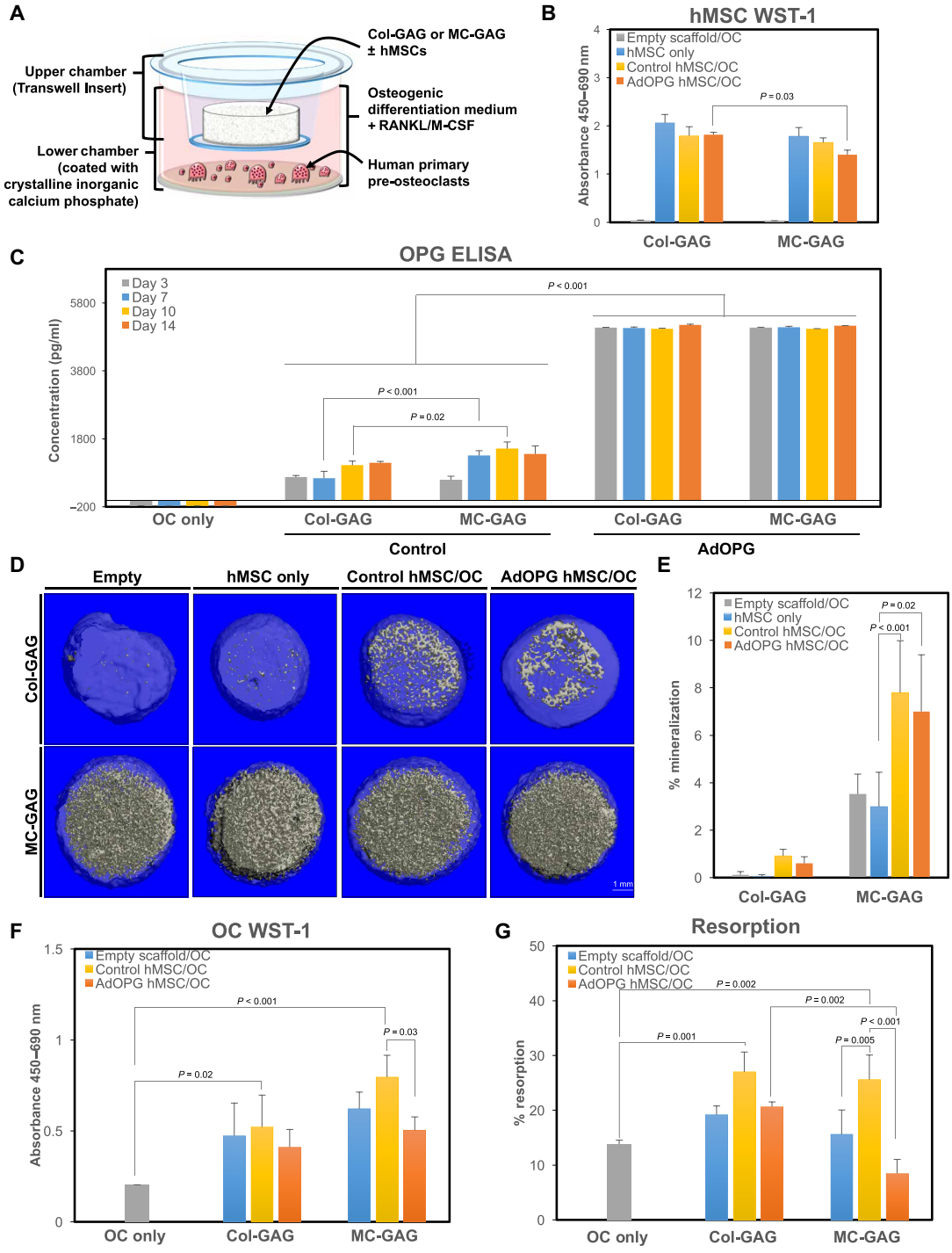

Fig. 4. Osteoclast cocultures indirectly augment mineralization in hMSCs undergoing mineralization on MC-GAG. (**A**) Schematic diagram of coculture design indicating the placement of differentiating hMSCs on Col-GAG or MC-GAG within Transwell insert and lower chamber consisting of primary pre-osteoclasts cultured on a plate coated with calcium phosphate to allow for the detection of resorptive pit activity. (**B**) WST-1 assays of hMSCs in single culture (hMSC only) or cocultured (control hMSC/OC and AdOPG hMSC/OC, respectively) on Col-GAG or MC-GAG for 21 days. Empty cell-free scaffolds cocultured with osteoclasts shown for control (empty scaffolds/OC). (**C**) OPG ELISA of hMSC/OC coculture medium (days 3, 7, 10, and 14) with control and AdOPG-transduced hMSCs on Col-GAG and MC-GAG. Differentiated osteoclast-only (OC only) culture shown at the left as a control. (**D**) Representative μCT images and (**E**) quantitative analysis of empty scaffold (empty), hMSCs without osteoclasts (hMSC only), control hMSCs cocultured with osteoclasts, or AdOPG-transduced hMSCs cocultured with osteoclasts on Col-GAG or MC-GAG for 21 days. (**F**) WST-1 assays of primary pre-osteoclasts in single culture (OC only), cocultured with empty scaffolds, or cocultured with control or AdOPG-transduced hMSCs (control hMSC and AdOPG hMSC, respectively) in medium supplemented with RANKL and M-CSF on Col-GAG or MC-GAG for 14 days. (**G**) Quantitative analysis of pit assays as the percentage of total area of well in differentiated osteoclasts without hMSCs (OC only) and osteoclasts cocultured with Col-GAG and MC-GAG as empty scaffolds, scaffolds with control hMSCs, and scaffolds with AdOPG-transduced hMSCs. Significant post hoc comparisons following ANOVA indicated with *P* values.

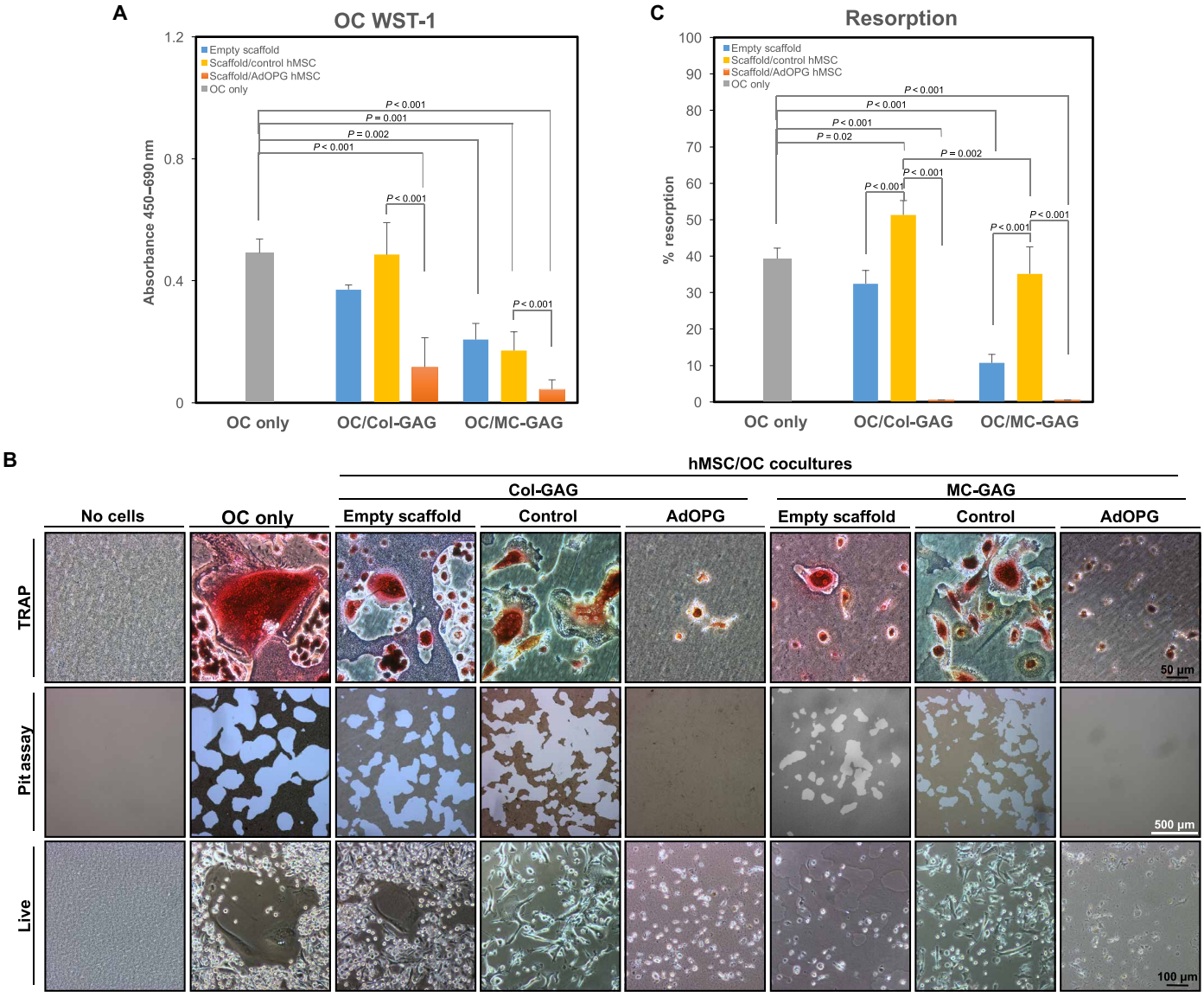

Fig. 5. AdOPG-infected hMSCs on Col-GAG and MC-GAG diminish the proliferation and resorption activity of osteoclasts. (**A**) WST-1 proliferation and viability assays of primary pre-osteoclasts in single culture (OC only), cocultured with empty scaffolds, or cocultured with control or AdOPG-transduced hMSCs (control hMSC and AdOPG hMSC, respectively) in medium supplemented with RANKL and M-CSF on Col-GAG or MC-GAG for 14 days. (**B**) TRAP staining (top row), resorption pits (middle row), and live images (bottom row) of negative control without cells (no cells), osteoclast only without hMSCs or scaffolds (OC only), and osteoclasts cocultured with Col-GAG or MC-GAG as empty scaffolds (empty scaffold), with control hMSCs (control), or with AdOPG-transduced hMSCs (AdOPG). (**C**) Quantitative analysis of pit assays as percentage of total area of well in differentiated osteoclasts without hMSCs (OC only) and osteoclasts cocultured with Col-GAG and MC-GAG as empty scaffolds, scaffolds with control hMSCs, and scaffolds with AdOPG-transduced hMSCs. Significant post hoc comparisons following ANOVA indicated with *P* values.

[$F(6,14) = 88.22$, $P < 0.001$; Fig. 5C]. In post hoc comparisons, no statistically significant differences were seen between osteoclasts cultured alone (OC only) and osteoclasts cocultured with empty Col-GAG, whereas osteoclasts cultured with empty MC-GAG were significantly less active ($P < 0.001$). In cocultures with control hMSCs differentiated on Col-GAG or MC-GAG, resorption increased compared to empty scaffolds ($P < 0.001$ for both), although the quantity of resorption continued to be lower in MC-GAG compared to Col-GAG ($P = 0.002$). In the presence of AdOPG, resorption was completely eliminated for either material compared to scaffolds with control hMSCs ($P < 0.001$ for both).

AdOPG transduction augments mineralization and hMSC expression of p-Smad1/5, Runx2, and p-ERK1/2 when directly contacting osteoclasts

Direct contact of hMSCs differentiated on Col-GAG and MC-GAG with hOCs allows for investigation of the net effects of positive and negative regulation including resorption on mineralization. Empty Col-GAG and MC-GAG scaffolds, scaffolds seeded with control hMSCs, or AdOPG-transduced hMSCs were directly cocultured with hOCs and concurrently differentiated for 14 days. Scaffolds were assessed for mineralization and activation of intracellular mediators known to be involved in osteogenic differentiation (Fig. 6).

Unlike indirect cocultures, direct cocultures with hOCs resulted in a decrease in mineral content on both Col-GAG and MC-GAG with control hMSCs when compared to empty scaffolds (Fig. 6, A and B). The decrease in mineralization is in concordance with the increase in hOC activity (Fig. 5, B and C) seen in the presence of hMSCs, as well as the presence of hOCs directly on the scaffolds (fig. S1). When hMSCs transduced with AdOPG on Col-GAG and MC-GAG were directly cocultured with hOCs, mineralization was significantly improved, resulting in a net osteogenic state.

To compare the osteogenic mechanisms activated in hMSCs in the direct coculture system, intracellular mediators known to be up-regulated in osteogenic differentiation were evaluated on Western blot analysis (Fig. 6C). Unlike single cultures with hMSCs, direct cocultures resulted in an up-regulation of p-Smad1/5, p-ERK1/2 (phosphorylated extracellular regulated kinase 1/2), and Runx2. These data suggest that hOCs simultaneously positively regulate hMSC osteogenesis while actively resorbing mineralized volumes. These activities may be separated using an endogenous secreted decoy receptor for RANKL.

DISCUSSION

In this work, we investigated the feasibility of combining OPG with a mineralized collagen scaffold for affecting osteogenic differentiation with concurrent osteoclastogenic inhibition. Using an adenoviral vector, we demonstrated that OPG expression did not affect the viability or proliferation of primary hMSCs and that expression could be detected at even 8 weeks following transduction. With respect to endogenous RANKL and OPG, hMSCs in MC-GAG scaffolds demonstrated a significantly lower RANKL/OPG cellular and scaffold-bound protein expression ratio compared to nonmineralized Col-GAG scaffolds, albeit a higher RANKL/OPG-secreted protein ratio. In the presence of AdOPG, the RANKL/OPG cellular and scaffold-bound protein expression ratios were significantly lowered from baseline. While AdOPG mildly reduced the secreted RANKL/OPG protein ratio in Col-GAG, AdOPG significantly diminished the secreted RANKL/OPG ratio in MC-GAG. Osteogenic differentiation of control versus AdOPG-transduced hMSCs did not show significant differences in terms of expression of osteogenic genes, p-Smad1/5, or quantitative matrix mineralization in the absence of osteoclasts. In the presence of differentiating primary hOCs in indirect cocultures, mineralization was increased beyond hMSC single cultures, particularly in hMSCs cultured on MC-GAG scaffolds. Augmented mineralization by hOCs persisted even with AdOPG transduction in indirect cocultures, suggesting that paracrine effects were responsible for the positive regulation. AdOPG transduction mildly affected hOC-mediated resorption in the presence of Col-GAG in indirect cultures, whereas resorption is significantly reduced in the presence of MC-GAG. Upon direct contact of differentiating osteoclasts with Col-GAG or MC-GAG materials, resorptive activities decreased but could be partially rescued with the addition of hMSCs. In the same direct cocultures with AdOPG-transduced hMSCs, the resorptive activities of osteoclasts were completely abrogated. The decrease in hOC resorptive activity by AdOPG resulted in an increase in activation of intracellular osteogenic mediators on both Col-GAG and MC-GAG scaffolds. These results suggest several conclusions: (i) hMSC osteogenic differentiation on MC-GAG scaffolds is largely unaffected by the addition of OPG; (ii) osteoclast and hMSCs cocultures positively regulate the activities of each other; (iii) OPG is largely sequestered on the scaffold, and thus, anti-osteoclastogenic effects are most evident in direct cocultures; and (iv) direct osteogenic and osteoclastogenic coupling may be separated to augment bone regeneration, where we observe that hMSCs on MC-GAG scaffolds combined with OPG augment osteoclast activity inhibition.

Two other groups have suggested that bone regeneration with OPG is a viable strategy. Su *et al.* (*28*) expressed OPG in rabbit periodontal ligament stem cells seeded on β-tricalcium phosphate materials for regeneration of alveolar defects and demonstrated improved bone healing. Liu *et al.* (*29*) reported using adenoviral expression of OPG in rat BMSCs implanted on hydroxyapatite scaffolds for repair of osteoporotic mandible defects. Similar to our current report, they reported long-lasting OPG expression, even after 6 weeks for their in vivo experiments with a statistically significant improvement in mineralization and decrease in osteoclast cell density. Our current work now contributes to the concept of OPG expression in primary human MSCs and its effect on primary hOC differentiation and activity. Our work also demonstrates that the expression of OPG does not diminish osteoclast-induced mineralization, suggesting that separate processes within the osteoclast control the paracrine stimulation of osteoprogenitors versus the resorptive activity of the osteoclast.

In part, the concept of blocking osteoclastogenesis is contrary to some of the lessons learned in the genetics literature. In OPG knockout mice, a recent study documented that the release of negative regulation in osteoclastogenesis coincided with a simultaneous increase in bone formation, which was mediated through the suppression of sclerostin expression (*30*). Conversely, Runx2/Cbfa1 (core-binding factor α1) knockout mouse studies indicated that maturational arrest in osteoblast differentiation also resulted in the absence of osteoclasts (*31*, *32*). Although this phenomenon was related to the expression of RANKL by osteoblasts downstream of Runx2, $Runx2^{-/-}$ mice with a soluble RANKL transgene did not result in complete rescue (*31*). The combination of these genetic studies indicates that a direct relationship exists between bone formation and resorption. Our current study reflects the positive coordination of osteogenic and osteoclastogenic differentiation with observed dual increases when both cell types are allowed to interact in coculture (Figs. 4 and 5). Thus, it is clear that systemic or permanent deficiencies of any of these factors are likely not necessary or useful for bone regeneration.

In normal physiology and pathology, there are many examples of transient changes in the relative abundance of positive or negative regulators of osteogenesis or osteoclastogenesis. For osteoclast activation and activity, the relative balance between RANKL and OPG has been suggested to be responsible for the net effect toward bone formation or resorption on the locoregional or organismal environment (*33*, *34*). In an effort to better understand fracture healing, Kon *et al.* (*35*) evaluated gene expression of the RANK/RANKL/OPG axis and proinflammatory cytokines in a mouse model. While OPG was constitutively expressed, RANKL was up-regulated in response to injury. Expressed in a different manner, Tanaka and colleagues (*36*) have demonstrated that the RANKL/OPG ratio changes over time following injury with a low ratio in the early stages, favoring bone formation, followed by a higher ratio, favoring bone resorption, later after injury. In our current work, there was a clear difference in the total endogenous OPG secreted (Fig. 4C), the endogenous RANKL/OPG protein ratio (Fig. 2E), and hOC resorptive

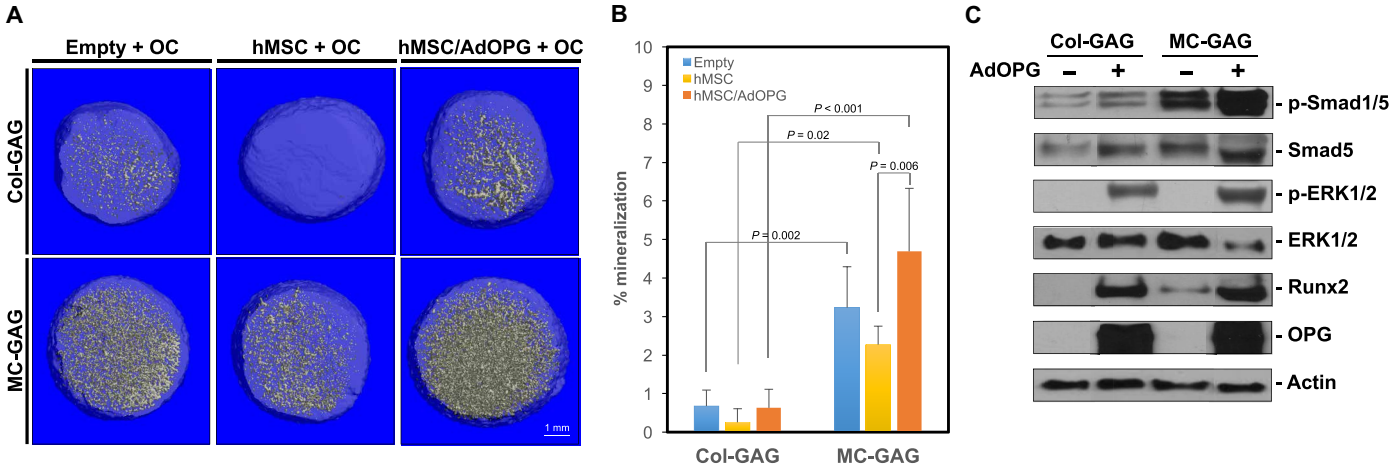

Fig. 6. Direct cocultures of osteoclasts with AdOPG-infected hMSCs on Col-GAG and MC-GAG increase p-Smad1/5, Runx2, p-ERK1/2, and mineralization. (**A**) Representative μCT images and (**B**) quantitative analysis of direct cocultures of osteoclasts with empty scaffold (empty + OC), control hMSCs (hMSC + OC), or AdOPG-transduced hMSCs (hMSC/AdOPG + OC) on Col-GAG or MC-GAG for 14 days. Significant post hoc comparisons following ANOVA indicated with *P* values. (**C**) Western blot of control of AdOPG-transduced primary hMSCs differentiated on Col-GAG or MC-GAG materials cocultured with osteoclasts for 14 days.

activity (Fig. 5C) between control hMSCs cultured in nonmineralized Col-GAG versus MC-GAG scaffolds. The addition of AdOPG increases the total quantity of OPG protein and diminishes the total cellular and scaffold-bound RANKL/OPG ratio corresponding to the decrease in osteoclast resorptive activity in both materials. The differences in hOC resorptive abilities between indirect and direct cocultures suggest that most of the OPG remain sequestered on the scaffold, potentially pointing toward the ability for spatial control of modulatory factors in the presence of Col-GAG materials. The addition of OPG decreased osteoclast resorption without losing the osteogenic effects of hOCs (Fig. 5, D and E). As the osteogenic stimulation of hOCs is evident in indirect cultures, paracrine signals are likely the main positive regulatory signals from hOCs.

Despite the bidirectional positive regulation of osteogenic and osteoclastogenic differentiation in coculture, the net effects of the direct cocultures were tipped toward resorption in the presence of endogenous hMSCs (Fig. 6, A and B), suggesting that the endogenous levels of OPG cannot overcome the osteoclast activation present in cocultures. In the presence of AdOPG, not only did mineralization improve Smad1/5 phosphorylation and Runx2 protein expression both increased. As this increase was not detected in single cultures of hMSCs transduced with AdOPG, these effects are most likely to be attributable to hOC-induced osteogenic effects. Similar to the paracrine effects on mineralization, cocultures of AdOPG-transduced hMSCs on MC-GAG with hOCs may diminish hOC-mediated resorptive capacities but do not mitigate the osteoinductive signals from hOCs.

One of the potential benefits of using OPG as a temporary measure in decreasing osteoclast activity is that its function is a nonsignaling, decoy receptor for the major osteoclast growth factor (*1*). Although we used an adenoviral vector for OPG expression because of its high efficiency and high protein production for the purposes of proof of concept, a nongenetic method for OPG delivery would likely be better suited for clinical translation for safety reasons. In addition, we detected a high level of OPG protein even at 8 weeks following transduction. This may represent a second drawback in using a genetic methodology for OPG delivery, as the remodeling phase of bone regeneration should be well underway at 8 weeks. Future work on the augmentation of osteoclast inhibition on MC-GAG materials would likely require refinement of the quantity and timing of OPG release.

In all, controlled coordination of both positive and negative processes is essential to the success of regenerative technologies. While most of the attention within the bone regeneration field has been focused on improving osteogenesis, consideration for diminishing osteoclastogenesis has only been recently investigated. Our current work details the ability of adenoviral expression of OPG in combination with MC-GAG to augment the inhibition of osteoclast resorptive activity without diminishing the positive paracrine effects on osteogenic differentiation. These findings contribute the potential utility of a strategy that capitalizes on a transient disturbance in osteoclast resorption to allow for the establishment of a critical mass of regenerated bone, suggesting new avenues for material development.

MATERIALS AND METHODS

Fabrication and chemical cross-linking of nonmineralized and mineralized collagen scaffolds

Col-GAG and MC-GAG scaffolds were prepared using lyophilization, as described previously (*37*–*39*). Briefly, microfibrillar, type I collagen (Collagen Matrix, Oakland, NJ) and chondroitin-6-sulfate (Sigma-Aldrich, St. Louis, MO) were combined in suspension in the absence and presence of calcium salts (calcium nitrate hydrate, $Ca(NO_3)_2{\cdot}4H_2O$; calcium hydroxide, $Ca(OH)_2$; Sigma-Aldrich, St. Louis, MO) in an acetic acid (Col-GAG) or phosphoric acid (MC-GAG) solution. Using a constant cooling rate technique at a rate of 1°C/min, the solution was frozen from room temperature to −10°C using a freeze dryer (Genesis, VirTis). Following sublimation of the ice phase, scaffolds were sterilized via ethylene oxide and cut into 8-mm disks in diameter and 4 mm in height for culture.

Cross-linking of scaffolds was performed after rehydration in phosphate-buffered saline (PBS) for 4 hours using 1-ethyl-3-(3-dimethylaminopropyl)carbodiimide (EDAC; Sigma-Aldrich) and *N*-hydroxysuccinimide (NHS; Sigma-Aldrich) at a molar ratio of 5:2:1 EDAC:NHS:COOH, where COOH represents the amount of

collagen in the scaffold as we previously described (*40*). Scaffolds were washed with PBS to remove any of the residual chemical.

Cell culture

Primary hMSCs (Lonza Inc., Allendale, NJ) were expanded in proliferation medium composed of Dulbecco's modified Eagle's medium (DMEM; Corning Cellgro, Manassas, VA) supplemented with 10% fetal bovine serum (Atlanta Biologicals, Atlanta, GA), 2 mM L-glutamine (Life Technologies, Carlsbad, CA), and penicillin (100 IU/ml)/streptomycin (100 μg/ml; Life Technologies).

2D culture

hMSCs of passage 3 to 5 were plated at 5000 cells per well in 12-well plates, grown until 80 to 90% confluent, and then transduced with and without an AdOPG and RFP in DMEM at a MOI of 200 and polybrene (4 μg/ml; Sigma-Aldrich, St. Louis, MO). Twenty-four hours after transduction, hMSCs were subjected to differentiation medium consisting of proliferation medium plus 10 mM β-glycerophosphate, ascorbic acid (50 μg/ml), and 0.1 μM dexamethasone. Cell cultures were evaluated on day 7 after transduction for morphological changes, transduction efficiency, and Western blot.

Osteogenic differentiation of hMSCs on Col-GAG and MC-GAG

hMSCs (3×10^5) were seeded onto 8-mm discs of CG-GAG and MC-GAG scaffolds in proliferation medium. The cells were resuspended in growth medium, and half of the suspension was used to seed one side of the scaffold. After incubation for 15 min, the scaffold was turned upside down and the other half of the suspension was used to seed the opposite side. One millimeter of growth medium was then added to each well. Twenty-four hours after seeding, the medium was switched to osteogenic differentiation medium consisting of 10 mM β-glycerophosphate, ascorbic acid (50 μg/ml), and 0.1 μM dexamethasone.

Indirect hMSC and hOC cocultures

hMSCs (2×10^5) were seeded to 6 mm of Col-GAG and MC-GAG scaffolds in proliferation medium. Twenty-four hours after seeding hMSCs, primary hOC precursors (6×10^4; Lonza Inc., Allendale, NJ) were cultured in Osteoclast Precursor Basal Medium (Lonza, Allendale NJ) supplemented with M-CSF (33 ng/ml), RANKL (66 ng/ml), 10 mM β-glycerophosphate, ascorbic acid (50 μg/ml), and 0.1 μM dexamethasone for concurrent hMSC and hOC differentiation on 24-well Corning Osteo Assay Surface Microplates (Corning, NY). After 2 hours, Col-GAG and MC-GAG scaffolds were transferred to 8-μm Transwell inserts (Corning, NY) and cocultured with hOCs. Medium was changed every 3 days for 3 weeks.

Direct hMSC and hOC cocultures

hMSCs (3.5×10^5) were seeded to 8 mm of Col-GAG and MC-GAG scaffolds in proliferation medium. Twenty-four hours after seeding hMSCs, hOCs (6×10^4) were cultured in Osteoclast Precursor Basal Medium (Lonza Inc., Allendale NJ) supplemented with M-CSF (33 ng/ml), RANKL (66 ng/ml), 10 mM β-glycerophosphate, ascorbic acid (50 μg/ml), and 0.1 μM dexamethasone on 24-well Osteo Assay Microplates. After 2 hours, Col-GAG and MC-GAG scaffolds were transferred to the Osteo Assay Microplates and directly cocultured with hOCs. Medium was changed every 3 days for 2 weeks.

Quantitative real-time reverse transcription polymerase chain reaction

RNeasy kit (Qiagen, Valencia, CA) was used to extract total RNA from scaffolds at 0, 3, and 14 days of culture. Gene sequences for 18S, Runx2, OPN, OPG, and receptor activator of RANKL were obtained from the National Center for Biotechnology Information gene database, and primers were designed (table S1). qRT-PCR was performed on the Opticon Continuous Fluorescence System (Bio-Rad Laboratories Inc., Hercules, CA) using the QuantiTect SYBR Green RT-PCR Kit (Qiagen). Cycle conditions were as follows: reverse transcription at 50°C (30 min); activation of HotStarTaq DNA polymerase/inactivation of reverse transcriptase at 95°C (15 min); and 45 cycles of 94°, 58°, and 72°C for 15, 30, and 45 s, respectively. Results were analyzed and presented as representative graphs of triplicate experiments.

Enzyme-linked immunosorbent assay

Supernatants were collected from hMSC only, osteoclast (OC) only, or hMSC and hOC cocultures. OPG protein concentrations were determined using the Human OPG DuoSet ELISA Kit (R&D Systems, Minneapolis, MN) according to the manufacturer's instructions. Briefly, a 96-well microplate was coated with the capture antibody and incubated overnight at room temperature. After blocking, samples were incubated for 2 hours at room temperature with the detection antibody, followed by incubation with streptavidin-horseradish peroxidase (HRP) for 20 min. The reaction was quenched by adding 100 μl of 2 N H_2SO_4. Plates were read at 450- and 540-nm wavelengths on the Epoch Microplate Reader (BioTex, Winooski, VT).

μCT imaging

Scaffolds were fixed using 10% formalin, and mineralization was quantified by μCT imaging using Scanco 35 (Scanco Medical AG, Bruttisellen, Switzerland) in triplicate for each time point. Scans were performed at medium resolution with a source voltage *E* of 70 kVp and with a current *I* of 114 μA. The images had a final element size of 12.5 μm. Images were analyzed using software supplied from Scanco (Image Processing Language version 5.6) and reconstructed into 3D volumes of interest. Optimum arbitrary threshold values of 20 (containing scaffold and mineralization) and 80 (containing mineralization alone) were used uniformly for all specimens to quantify mineralized areas from surrounding unmineralized scaffold. Analysis of 3D reconstructions was performed using Scanco Evaluation script no. 2 (3D segmentation of two volumes of interest: solid dense in transparent low-density object) and script no. 6 (bone volume/density-only bone evaluation) for volume determinations.

Western blot

Total protein lysates were prepared from scaffolds at 0, 3, 14, 28, 42, and 56 days of culture by incubating scaffolds morselized using scissors in 3× SDS reducing sample buffer. Lysates were then incubated at 95°C for 5 min and centrifuged in 0.2 μm of Spin-X filters (Corning Costar, Corning, NY) at 14,000 rpm for 5 min. Protein concentration was measured, and equal amounts were subjected to 4 to 20% SDS–polyacrylamide gel electrophoresis (Bio-Rad, Hercules, CA). Western blot analysis was carried out with antibodies against OPG, RANKL, p-Smad1/5, total Smad5, p-ERK1/2, total ERK1/2, and β-actin, followed by 1:4000 dilutions of HRP-conjugated immunoglobulin G antibodies (Bio-Rad, Hercules, CA) and an enhanced chemiluminescent substrate (Thermo Fisher Scientific, Rockford, IL). For the detection of p-Smad1/5 and total Smad5, 10 μg of lysate was loaded per lane. For the detection of OPG, RANKL, p-ERK1/2, total ERK1/2, and β-actin, 20 μg of lysate was loaded per lane. All antibodies were obtained from Cell Signaling Technology (Danvers, MA), with the exception of RANKL, OPG, and β-actin antibodies from

Santa Cruz Biotechnology (Santa Cruz, CA). Imaging analysis was carried out using ImageJ (NIH, Bethesda, MD). The RANKL/OPG-relative protein ratios were calculated by quantifying the densitometry of all RANKL and OPG normalized to actin using ImageJ (NIH, Bethesda, MA).

WST-1 assay

Culture medium was supplemented with cell proliferation reagent WST-1 (Roche, Basel, Switzerland) at a 1:10 concentration. Scaffolds were incubated for 3 to 4 hours at 37°C in a humidified atmosphere with 5% CO_2. Absorbance of the incubation medium was measured at 450 and 690 nm (Epoch spectrophotometer, BioTek, Winooski, VT).

TRAP staining

hOCs were detected using the Leukocyte TRAP Kit 387-A (Sigma-Aldrich) according to the manufacturer's instructions. Briefly, cultured cells were fixed with formaldehyde for 5 min at room temperature, washed, and air-dried. After staining, TRAP-positive multinucleated cells were observed under a phase-contrast microscope at 20× magnification and digitally photographed.

Resorption pit assay

Activity of hOCs in single culture or cocultured with scaffolds with and without hMSCs was evaluated for resorption pit formation on Osteo Assay Microplates. At the completion of the culture period, culture medium was aspirated, and 500 µl of 10% bleach solution was added for 5 min at room temperature. The wells were washed with distilled water and allowed to dry at room temperature for 3 to 5 hours. Pits were observed using a standard microscope and digitally photographed. The percentage of resorption for the whole well of the culture at magnification 2× was calculated by ImageJ.

Statistical analysis

All statistical analyses were performed using SPSS version 24 (Chicago, IL). Data points were composed of duplicates of at least three independent experiments, unless otherwise indicated. Mean measurements of mRNA expression were analyzed for statistical significance by ANOVA, followed by post hoc tests using the Tukey's criterion. A value of $P < 0.05$ was considered significant.

SUPPLEMENTARY MATERIALS

Supplementary material for this article is available at http://advances.sciencemag.org/cgi/content/full/5/6/eaaw4991/DC1

Supplementary Materials and Methods

Table S1. Primer sequences.

Fig. S1. Osteoclasts migrate into Col-GAG and MC-GAG scaffolds in the presence of control hMSCs in direct cocultures.

REFERENCES AND NOTES

1. J. B. Maxhimer, J. P. Bradley, J. C. Lee, Signaling pathways in osteogenesis and osteoclastogenesis: Lessons from cranial sutures and applications to regenerative medicine. *Genes Dis.* **2**, 57–68 (2015).
2. J. C. Lee, L. Spiguel, D. S. Shenaq, M. Zhong, C. Wietholt, T.-C. He, R. R. Reid, Role of RANK-RANKL-OPG axis in cranial suture homeostasis. *J. Craniofac. Surg.* **22**, 699–705 (2011).
3. D. M. Anderson, E. Maraskovsky, W. L. Billingsley, W. C. Dougall, M. E. Tometsko, E. R. Roux, M. C. Teepe, R. F. DuBose, D. Cosman, L. Galibert, A homologue of the TNF receptor and its ligand enhance T-cell growth and dendritic-cell function. *Nature* **390**, 175–179 (1997).
4. Y.-Y. Kong, H. Yoshida, I. Sarosi, H.-L. Tan, E. Timms, C. Capparelli, S. Morony, A. J. Oliveira-dos-Santos, G. van, A. Itie, W. Khoo, A. Wakeham, C. R. Dunstan, D. L. Lacey, T. W. Mak, W. J. Boyle, J. M. Penninger, OPGL is a key regulator of osteoclastogenesis, lymphocyte development and lymph-node organogenesis. *Nature* **397**, 315–323 (1999).
5. J. Li, I. Sarosi, X.-Q. Yan, S. Morony, C. Capparelli, H.-L. Tan, S. McCabe, R. Elliott, S. Scully, G. van, S. Kaufman, S.-C. Juan, Y. Sun, J. Tarpley, L. Martin, K. Christensen, J. McCabe, P. Kostenuik, H. Hsu, F. Fletcher, C. R. Dunstan, D. L. Lacey, W. J. Boyle, RANK is the intrinsic hematopoietic cell surface receptor that controls osteoclastogenesis and regulation of bone mass and calcium metabolism. *Proc. Natl. Acad. Sci. U.S.A.* **97**, 1566–1571 (2000).
6. T. J. Yun, M. D. Tallquist, A. Aicher, K. L. Rafferty, A. J. Marshall, J. J. Moon, M. K. Ewings, M. Mohaupt, S. W. Herring, E. A. Clark, Osteoprotegerin, a crucial regulator of bone metabolism, also regulates B cell development and function. *J. Immunol.* **166**, 1482–1491 (2001).
7. W. S. Simonet, D. L. Lacey, C. R. Dunstan, M. Kelley, M.-S. Chang, R. Lüthy, H. Q. Nguyen, S. Wooden, L. Bennett, T. Boone, G. Shimamoto, M. DeRose, R. Elliott, A. Colombero, H.-L. Tan, G. Trail, J. Sullivan, E. Davy, N. Bucay, L. Renshaw-Gegg, T. M. Hughes, D. Hill, W. Pattison, P. Campbell, S. Sander, G. van, J. Tarpley, P. Derby, R. Lee, W. J. Boyle, Osteoprotegerin: A novel secreted protein involved in the regulation of bone density. *Cell* **89**, 309–319 (1997).
8. L. M. Flick, J. M. Weaver, M. Ulrich-Vinther, F. Abuzzahab, X. Zhang, W. C. Dougall, D. Anderson, R. J. O'Keefe, E. M. Schwarz, Effects of receptor activator of NFκB (RANK) signaling blockade on fracture healing. *J. Orthop. Res.* **21**, 676–684 (2003).
9. A. D. Barrow, N. Raynal, T. L. Andersen, D. A. Slatter, D. Bihan, N. Pugh, M. Cella, T. Kim, J. Rho, T. Negishi-Koga, J.-M. Delaisse, H. Takayanagi, J. Lorenzo, M. Colonna, R. W. Farndale, Y. Choi, J. Trowsdale, OSCAR is a collagen receptor that costimulates osteoclastogenesis in DAP12-deficient humans and mice. *J. Clin. Invest.* **121**, 3505–3516 (2011).
10. S. Herman, R. B. Müller, G. Krönke, J. Zwerina, K. Redlich, A. J. Hueber, H. Gelse, E. Neumann, U. Müller-Ladner, G. Schett, Induction of osteoclast-associated receptor, a key osteoclast costimulation molecule, in rheumatoid arthritis. *Arthritis Rheum.* **58**, 3041–3050 (2008).
11. J. C. Lee, E. J. Volpicelli, Bioinspired collagen scaffolds in cranial bone regeneration: From bedside to bench. *Adv. Healthc. Mater.* 10.1002/adhm.201700232 (2017).
12. J. Salbach-Hirsch, N. Ziegler, S. Thiele, S. Moeller, M. Schnabelrauch, V. Hintze, D. Scharnweber, M. Rauner, L. C. Hofbauer, Sulfated glycosaminoglycans support osteoblast functions and concurrently suppress osteoclasts. *J. Cell. Biochem.* **115**, 1101–1111 (2014).
13. A. Miyauchi, K. A. Hruska, E. M. Greenfield, R. Duncan, J. Alvarez, R. Barattolo, S. Colucci, A. Zambonin-Zallone, S. L. Teitelbaum, A. Teti, Osteoclast cytosolic calcium, regulated by voltage-gated calcium channels and extracellular calcium, controls podosome assembly and bone resorption. *J. Cell Biol.* **111**, 2543–2552 (1990).
14. A. Mozar, N. Haren, M. Chasseraud, L. Louvet, C. Mazière, A. Wattel, R. Mentaverri, P. Morlière, S. Kamel, M. Brazier, J. C. Mazière, Z. A. Massy, High extracellular inorganic phosphate concentration inhibits RANK-RANKL signaling in osteoclast-like cells. *J. Cell. Physiol.* **215**, 47–54 (2008).
15. Y. R. Shih, Y. Hwang, A. Phadke, H. Kang, N. S. Hwang, E. J. Caro, S. Nguyen, M. Siu, E. A. Theodorakis, N. C. Gianneschi, K. S. Vecchio, S. Chien, O. K. Lee, S. Varghese, Calcium phosphate-bearing matrices induce osteogenic differentiation of stem cells through adenosine signaling. *Proc. Natl. Acad. Sci. U.S.A.* **111**, 990–995 (2014).
16. H. D. Kim, H. L. Jang, H.-Y. Ahn, H. K. Lee, J. Park, E.-s. Lee, E. A. Lee, Y.-H. Jeong, D.-G. Kim, K. T. Nam, N. S. Hwang, Biomimetic whitlockite inorganic nanoparticles-mediated in situ remodeling and rapid bone regeneration. *Biomaterials* **112**, 31–43 (2017).
17. K. Jiao, L.-n. Niu, Q.-h. Li, F.-m. Chen, W. Zhao, J.-j. Li, J. H. Chen, C. W. Cutler, D. H. Pashley, F. R. Tay, Biphasic silica/apatite co-mineralized collagen scaffolds stimulate osteogenesis and inhibit RANKL-mediated osteoclastogenesis. *Acta Biomater.* **19**, 23–32 (2015).
18. J. C. Lee, C. T. Pereira, X. Ren, W. Huang, D. Bischoff, D. W. Weisgerber, D. T. Yamaguchi, B. A. Harley, T. A. Miller, Optimizing collagen scaffolds for bone engineering: Effects of cross-linking and mineral content on structural contraction and osteogenesis. *J. Craniofac. Surg.* **26**, 1992–1996 (2015).
19. X. Ren, D. Bischoff, D. W. Weisgerber, M. S. Lewis, V. Tu, D. T. Yamaguchi, T. A. Miller, B. A. C. Harley, J. C. Lee, Osteogenesis on nanoparticulate mineralized collagen scaffolds via autogenous activation of the canonical BMP receptor signaling pathway. *Biomaterials* **50**, 107–114 (2015).
20. X. Ren, D. W. Weisgerber, D. Bischoff, M. S. Lewis, R. R. Reid, T. C. He, D. T. Yamaguchi, T. A. Miller, B. A. C. Harley, J. C. Lee, Nanoparticulate mineralized collagen scaffolds and BMP-9 induce a long-term bone cartilage construct in human mesenchymal stem cells. *Adv. Healthc. Mater.* **5**, 1821–1830 (2016).
21. X. Ren, V. Tu, D. Bischoff, D. W. Weisgerber, M. S. Lewis, D. T. Yamaguchi, T. A. Miller, B. A. C. Harley, J. C. Lee, Nanoparticulate mineralized collagen scaffolds induce in vivo bone regeneration independent of progenitor cell loading or exogenous growth factor stimulation. *Biomaterials* **89**, 67–78 (2016).
22. Q. Zhou, X. Ren, D. Bischoff, D. W. Weisgerber, D. T. Yamaguchi, T. A. Miller, B. A. C. Harley, J. C. Lee, Nonmineralized and mineralized collagen scaffolds induce differential osteogenic signaling pathways in human mesenchymal stem cells. *Adv. Healthc. Mater.* **6**, 10.1002/adhm.201700641 (2017).

23. X. Ren, Q. Zhou, D. Foulad, M. J. Dewey, D. Bischoff, T. A. Miller, D. T. Yamaguchi, B. A. C. Harley, J. C. Lee, Nanoparticulate mineralized collagen glycosaminoglycan materials directly and indirectly inhibit osteoclastogenesis and osteoclast activation. *J. Tissue Eng. Regen. Med.* (2019).
24. S. K. Tat, J.-P. Pelletier, D. Lajeunesse, H. Fahmi, N. Duval, J. Martel-Pelletier, Differential modulation of RANKL isoforms by human osteoarthritic subchondral bone osteoblasts: Influence of osteotropic factors. *Bone* **43**, 284–291 (2008).
25. T. Ikeda, M. Kasai, J. Suzuki, H. Kuroyama, S. Seki, M. Utsuyama, K. Hirokawa, Multimerization of the receptor activator of nuclear factor-κB ligand (RANKL) isoforms and regulation of osteoclastogenesis. *J. Biol. Chem.* **278**, 47217–47222 (2003).
26. S. Palumbo, W.-J. Li, Osteoprotegerin enhances osteogenesis of human mesenchymal stem cells. *Tissue Eng. Part A* **19**, 2176–2187 (2013).
27. H. Yu, P. de Vos, Y. Ren, Overexpression of osteoprotegerin promotes preosteoblast differentiation to mature osteoblasts. *Angle Orthod.* **81**, 100–106 (2011).
28. F. Su, S.-S. Liu, J.-L. Ma, D.-S. Wang, L.-L. E, H.-C. Liu, Enhancement of periodontal tissue regeneration by transplantation of osteoprotegerin-engineered periodontal ligament stem cells. *Stem Cell Res. Ther.* **6**, 22 (2015).
29. X. Liu, C. Bao, H. H. K. Xu, J. Pan, J. Hu, P. Wang, E. Luo, Osteoprotegerin gene-modified BMSCs with hydroxyapatite scaffold for treating critical-sized mandibular defects in ovariectomized osteoporotic rats. *Acta Biomater.* **42**, 378–388 (2016).
30. M. Koide, Y. Kobayashi, T. Yamashita, S. Uehara, M. Nakamura, B. Y. Hiraoka, Y. Ozaki, T. Iimura, H. Yasuda, N. Takahashi, N. Udagawa, Bone formation is coupled to resorption via suppression of sclerostin expression by osteoclasts. *J. Bone Miner. Res.* **32**, 2074–2086 (2017).
31. H. Enomoto, S. Shiojiri, K. Hoshi, T. Furuichi, R. Fukuyama, C. A. Yoshida, N. Kanatani, R. Nakamura, A. Mizuno, A. Zanma, K. Yano, H. Yasuda, K. Higashio, K. Takada, T. Komori, Induction of osteoclast differentiation by Runx2 through receptor activator of nuclear factor-κB ligand (RANKL) and osteoprotegerin regulation and partial rescue of osteoclastogenesis in Runx2$^{-/-}$ mice by RANKL transgene. *J. Biol. Chem.* **278**, 23971–23977 (2003).
32. Y.-H. Gao, T. Shinki, T. Yuasa, H. Kataoka-Enomoto, T. Komori, T. Suda, A. Yamaguchi, Potential role of cbfa1, an essential transcriptional factor for osteoblast differentiation, in osteoclastogenesis: Regulation of mRNA expression of *osteoclast differentiation factor* (*ODF*). *Biochem. Biophys. Res. Commun.* **252**, 697–702 (1998).
33. B. Kadriu, P. W. Gold, D. A. Luckenbaugh, M. S. Lener, E. D. Ballard, M. J. Niciu, I. D. Henter, L. T. Park, R. T. De Sousa, P. Yuan, R. Machado-Vieira, C. A. Zarate, Acute ketamine administration corrects abnormal inflammatory bone markers in major depressive disorder. *Mol. Psychiatry* **23**, 1626–1631 (2017).
34. F. Gori, L. C. Hofbauer, C. R. Dunstan, T. C. Spelsberg, S. Khosla, B. L. Riggs, The expression of osteoprotegerin and RANK ligand and the support of osteoclast formation by stromal-osteoblast lineage cells is developmentally regulated. *Endocrinology* **141**, 4768–4776 (2000).
35. T. Kon, T. J. Cho, T. Aizawa, M. Yamazaki, N. Nooh, D. Graves, L. C. Gerstenfeld, T. A. Einhorn, Expression of osteoprotegerin, receptor activator of NF-κB ligand (osteoprotegerin ligand) and related proinflammatory cytokines during fracture healing. *J. Bone Miner. Res.* **16**, 1004–1014 (2001).
36. H. Tanaka, T. Mine, H. Ogasa, T. Taguchi, C. T. Liang, Expression of RANKL/OPG during bone remodeling in vivo. *Biochem. Biophys. Res. Commun.* **411**, 690–694 (2011).
37. B. A. Harley, A. K. Lynn, Z. Wissner-Gross, W. Bonfield, I. V. Yannas, L. J. Gibson, Design of a multiphase osteochondral scaffold. II. Fabrication of a mineralized collagen-glycosaminoglycan scaffold. *J. Biomed. Mater. Res. A* **92**, 1066–1077 (2010).
38. B. A. Harley, J. H. Leung, E. C. C. M. Silva, L. J. Gibson, Mechanical characterization of collagen-glycosaminoglycan scaffolds. *Acta Biomater.* **3**, 463–474 (2007).
39. D. W. Weisgerber, D. O. Kelkhoff, S. R. Caliari, B. A. Harley, The impact of discrete compartments of a multi-compartment collagen-GAG scaffold on overall construct biophysical properties. *J. Mech. Behav. Biomed. Mater.* **28**, 26–36 (2013).
40. L. H. Olde Damink, P. J. Dijkstra, M. J. A. van Luyn, P. B. van Wachem, P. Nieuwenhuis, J. Feijen, Cross-linking of dermal sheep collagen using a water-soluble carbodiimide. *Biomaterials* **17**, 765–773 (1996).

Acknowledgments

Funding: This work was supported by the U.S. Department of Veterans Affairs under award no. IK2 BX002442 (to J.C.L.), the Aramont Foundation (to T.A.M.), the Jean Perkins Foundation (to J.C.L.), and the Plastic Surgery Foundation under award no. 234813 (to J.C.L.). This work was supported by the Office of the Assistant Secretary of Defense for Health Affairs Broad Agency Announcement for Extramural Medical Research through the award no. W81XWH-16-1-0566 (to B.A.C.H.). Opinions, interpretations, conclusions, and recommendations are those of the authors and are not necessarily endorsed by the Department of Defense. Research reported in this publication was also supported by the National Institute of Dental and Craniofacial Research of the National Institutes of Health under award no. R21 DE026582 (to B.A.C.H.). The content is solely the responsibility of the authors and does not necessarily represent the official views of the National Institutes of Health. We are grateful for the funding for this study provided by the NSF Graduate Research Fellowship DGE-1144245 (to M.J.D.). **Author contributions:** J.C.L. designed the experiments and interpreted the data. Q.Z., X.R., D.F., and D.B. performed the experiments and assisted in the analysis of the data. A.S.T., M.J.D., and B.A.C.H. fabricated the scaffolds. R.R.R. and T.-C.H. provided the AdOPG. R.R.R., T.-C.H., D.T.Y., T.A.M., and B.A.C.H. contributed valuable comments at multiple stages of the study. J.C.L. and X.R. wrote the manuscript, and all authors contributed to review of the manuscript. **Competing interests:** J.C.L., B.A.C.H., X.R., and T.A.M. are inventors on a patent application related to this work filed by the University of California, Los Angeles (no. PCT/US2019/016709, filed 05 February 2019). All other authors declare that they have no competing interests. **Data and materials availability:** All data needed to evaluate the conclusions in the paper are present in the paper and/or the Supplementary Materials. Additional data related to this paper may be requested from the authors.

Submitted 27 December 2018
Accepted 3 May 2019
Published 12 June 2019
10.1126/sciadv.aaw4991

Citation: X. Ren, Q. Zhou, D. Foulad, A. S. Tiffany, M. J. Dewey, D. Bischoff, T. A. Miller, R. R. Reid, T.-C. He, D. T. Yamaguchi, B. A. C. Harley, J. C. Lee, activity without affecting osteogenesis on nanoparticulate mineralized collagen scaffolds. *Sci. Adv.* **5**, eaaw4991 (2019).